International Journal of Fracture **117:** 269–286, 2002.

An approximate, analytical approach to the 'HRR'-solution for sharp V-notches

S. FILIPPI[1], M. CIAVARELLA[2] and P. LAZZARIN[3,*]
[1]*Department of Mechanical Engineering - University of Padova, Via Venezia 1, 35100 Padova (Italy);*
[2]*CNR-IRIS, Computational Mechanics of Solids, Str. Crocefisso 2B, 70125 Bari (Italy);*
[3]*Department of Management and Engineering - University of Padova, Stradella S.Nicola 3, 36100 Vicenza (Italy);*
**Corresponding author (e-mail: plazzarin@gest.unipd.it)*

Received 9 March 2001; accepted in revised form 19 August 2002

Abstract. The well-known so-called 'HRR-solution' (Hutchinson, 1968 and Rice and Rosengren, 1968) considers the elasto-plastic stress field in a power-law strain hardening material near a sharp crack. It provides a closed form explicit expression for the stress singularity as a function of the power-law exponent 'n' of the material, but the stress angular variation functions are *not* found in closed form. More recently, similar formulations have appeared in the literature for sharp V-notches under mode I and II loading conditions. In such cases not only is the angular variation of the stress fields obtained numerically, but so is the singularity exponent of the stress field. In the present paper, approximate but accurate closed form solutions are first reported for sharp V-notches with an included angle greater than $\pi/6$ radians. Such solutions, limited here to Mode I loading conditions, allow a very satisfactory estimate of the angular stress components in the neighbourhood of the notch tip, in the entire range of notch angles and for the most significant values of n (i.e. from 1 to 15). When the notch opening angle tends towards zero, and the notch approaches the crack case, the solution becomes much more complex and a precise evaluation of the parameters involved requires a best-fitting procedure which, however, can be carried out in an automatic way. This solution is also reported in the paper and its degree of accuracy is discussed in detail.

Key words: HRR solution, V-Notch, elastoplastic stress distributions

1. Introduction

At the end of the '60s, HRR and J-integral theories were developed to set the entire basis of the modern Non-Linear (or Elasto-Plastic) Fracture Mechanics (NLFM, EPFM). (Rice, 1968, Hutchinson, 1968, and Rice and Rosengren, 1968). The starting point is the monotonic stress-strain constitutive law of many ductile solids undergoing uniaxial tension, i.e. the well known Ramberg-Osgood law $\varepsilon = \frac{\sigma}{E} + \left(\frac{\sigma}{A}\right)^n$, where E is Young's modulus, n is the strain hardening exponent (n=1 for linear elastic material, $n = \infty$ for elastic-perfectly plastic), and A is a material constant, the 'monotonic strength coefficient'. Near a crack tip, the stresses become very great and the elastic term can be neglected, so that we write $\frac{\varepsilon}{\varepsilon_y} = \alpha \left(\frac{\sigma}{\sigma_y}\right)^n$, where $\varepsilon_y = \sigma_y/E$; then, when generalized to multiaxial stress state under the 'J_2 deformation' (or 'total strain') theory (in order to simplify the mathematical treatment with respect to the more correct 'incremental' or 'flow' theories of plasticity), these become

$$\frac{\varepsilon_{ij}}{\varepsilon_y} = \frac{3\alpha}{2}\left(\frac{\sigma_e}{\sigma_y}\right)^{n-1}\frac{S_{ij}}{\sigma_y}; \quad \text{where } \sigma_e = \sqrt{\frac{3}{2}S_{ij}S_{ij}}$$

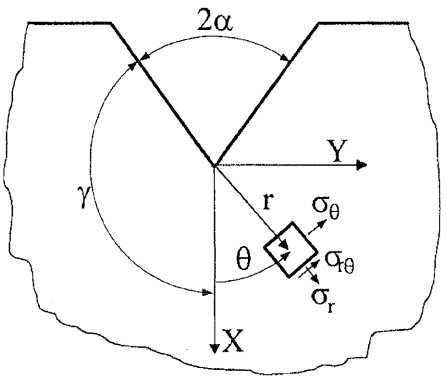

Figure 1. Notch geometry and coordinate system.

and S_{ij} are the deviatoric stress components. It is clear that the use of J_2 theory is only correct in cases of proportional loading, where the material behaves in all respects as a nonlinear elastic material; for significant non-proportional loading, deviations occur and the incremental flow theories of plasticity should be used. Rice and Rosengren (1968) then showed that the strength of the near-tip field is represented by the J-integral (equivalently to the K stress intensity factors of LEFM), that the stresses, strains and displacements exhibit $r^{-1/(n+1)}$, $r^{-n/(n+1)}$, $r^{1/(n+1)}$, respectively, and the 'HRR' fields can be represented still (as in the linear case) in separate variables in polar coordinates r,θ (as immediate consequence of self-similarity), and in particular

$$\sigma_{ij} = cr^{-s}\tilde{\sigma}_{ij}(\theta, n) \tag{1}$$

where $s=1/(n+1)$ is the singularity strength and c contains J-integral and a mild dependence on n (Hutchinson, 1968, Rice and Rosengren, 1968). The 'universal functions', $\tilde{\sigma}_{rr}$, $\tilde{\sigma}_{\theta\theta}$, $\tilde{\sigma}_{r\theta}$, depend on the state of stress (i.e. whether it is plane stress or plane strain) as well as n, but are not given in closed form.

Moving to the more general case of sharp V-notches, the problem becomes more demanding: not only are the angular 'universal functions' still not given in closed form, but even the singularity strength, s, requires a numerical solution as a function of n (Kuang and Xu, 1987, Xia and Wang, 1993, Yuan and Lin, 1994, Lazzarin et al. 2001). The formulation in fact leads to a system of differential equations that is generally solved with 'multi-shooting' techniques or, more recently, special FEM techniques (Zhang and Joseph, 1998, Chen and Ushijima, 2000).

As far as the authors are aware, technical literature lacks stress field expressions with a well documented degree of accuracy. In the present paper, an approximate closed form solution is developed for sharp V-notches, under a simplifying assumption on the governing system of differential equations, which is reduced to a treatable form.

2. Analytical background

Starting from the formulation proposed by Yuan and Lin (1994) - who were able to extend to V-notches a stress function approach previously used for cracks by Ponte Castañeda (1985) and Sharma and Aravas (1991, 1993) - the problem can be stated directly in terms of local

stresses and displacements (see Figure 1 for the reference system), leading to the following first order system of equations:

$$(1 - s)\tilde{\sigma}_{rr} - \tilde{\sigma}_{\theta\theta} + \tilde{\sigma}_{r\theta,\theta} = 0 \tag{2}$$

$$\tilde{\sigma}_{\theta\theta,\theta} + (2 - s)\tilde{\sigma}_{r\theta} = 0 \tag{3}$$

$$\tilde{u}_r + \tilde{u}_{\theta,\theta} - \frac{3}{2}\tilde{\sigma}_e^{n-1}\tilde{S}_{\theta\theta} = 0 \tag{4}$$

$$\frac{1}{2}(\tilde{u}_{r,\theta} - sn\tilde{u}_{\theta,\theta}) - \frac{3}{2}\tilde{\sigma}_e^{n-1}\tilde{\sigma}_{r\theta} = 0 \tag{5}$$

In (2–5), σ_e and S_{ij} are the Von Mises equivalent stress and the deviatoric components of the stress tensor. (For more details see Yuan and Lin (1994) as well as the leading order system in mixed load conditions recently reported by Lazzarin et al. (2001)). Also, under plane strain conditions, the following relations hold:

$$(1 - sn)\tilde{u}_r - \frac{3}{2}\tilde{\sigma}_e^{n-1}\tilde{S}_{rr} = 0 \tag{6}$$

$$\tilde{S}_{zz} = 0 \tag{7}$$

Let us then introduce the algebraic condition (6) into (4), and rewrite the differential system as a function of the stress components $\tilde{\sigma}_{rr}$, $\tilde{\sigma}_{\theta\theta}$, $\tilde{\theta}_{r\theta}$ and the displacement $\tilde{u}_\theta$.

$$(1 - s)\tilde{\sigma}_{rr} - \tilde{\sigma}_{\theta\theta} + \tilde{\sigma}_{r\theta,\theta} = 0 \tag{8}$$

$$\tilde{\sigma}_{\theta\theta,\theta} + (2 - s)\tilde{\sigma}_{r\theta} = 0 \tag{9}$$

$$\tilde{u}_{\theta,\theta} = \frac{3}{4}\tilde{\sigma}_1^{n-1}\frac{2 - sn}{1 - sn}(\tilde{\sigma}_{\theta\theta} - \tilde{\sigma}_{rr}) = 0 \tag{10}$$

$$\tilde{\sigma}_{rr,\theta} = \tilde{\sigma}_{\theta\theta,\theta} + \frac{4(1 - sn)\tilde{\sigma}_{r\theta} + \frac{4}{3}\tilde{\sigma}_e^{1-n}(1 - sn)sn\tilde{u}_\theta - 3(n - 1)\frac{\tilde{\sigma}_{rr} - \tilde{\sigma}_{\theta\theta}}{\tilde{\sigma}_e^2}\tilde{\sigma}_{r\theta}\tilde{\sigma}_{r\theta,\theta}}{1 + \frac{3}{4}(n - 1)\frac{(\tilde{\sigma}_{\theta\theta} - \tilde{\sigma}_{rr})^2}{\tilde{\sigma}_e^2}} \tag{11}$$

It is clear that while Equations (8, 9), which derive form the equilibrium conditions, are linear, Equations (10, 11) shows a complex dependence of the $\tilde{u}_{\theta,1}$ and $\tilde{\sigma}_{rr,\theta}$ terms on stress and displacement indexes. The system (8-11) does not allow a full analytical solution. We therefore proceed by simplifying the formulation in order to render the mathematics easier to dealt with. The range of applicability and the degree of accuracy of the new approximate solutions will be discussed in details.

3. A first-step simplified formulation

An approximate analytical approach is here proposed to simplify the first order problem previously stated in terms of local stresses and displacements. We observe that the boundary conditions for the symmetric mode are (see Figure 2):

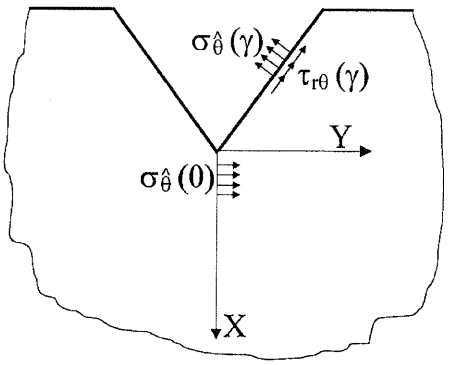

Figure 2. Boundary conditions on the notch.

$$\begin{aligned} &u_\theta(r, 0) = 0 \qquad \sigma_{\theta\theta}(r, \gamma) = 0 \\ &\sigma_{r\theta}(r, 0) \qquad \sigma_{r\theta}(r, \gamma) = 0 \end{aligned} \tag{12}$$

Manipulating these conditions we can also highlight the following characteristics:

$$\tilde{\sigma}_{r\theta,\theta}(\overline{\theta}) = 0 \tag{13}$$

$$\tilde{\sigma}_{rr}(\overline{\overline{\theta}}) - \tilde{\sigma}_{\theta\theta}(\overline{\overline{\theta}}) = 0 \tag{14}$$

Equation (13) comes directly from Rolle's theorem, given (12) for a $\overline{\theta}$ in the interval $(0, \gamma)$. Thanks to the equilibrium condition given by (8), it follows that $\tilde{\sigma}_{rr}(\overline{\theta}) - \tilde{\sigma}_{\theta\theta}(\overline{\theta}) > 0$ being s, $\tilde{\sigma}_{rr}(\overline{\theta})$, $\tilde{\sigma}_{\theta\theta}(\overline{\theta})$ all positive; moreover, numerical analysis shows that, except for the special case n=1, $\gamma = 0$, we have always $\tilde{\sigma}_{\theta\theta}(0) > \tilde{\sigma}_{rr}(0)$. There exists, therefore, an angle $\overline{\overline{\theta}}$ in the interval $(0, \overline{\theta})$ such that (14) is satisfied. Consequently, the expression

$$3(n-1)\frac{\tilde{\sigma}_{rr} - \tilde{\sigma}_{\theta\theta}}{\tilde{\sigma}_e^2}\tilde{\sigma}_{r\theta}\tilde{\sigma}_{r\theta,\theta} \tag{15}$$

is zero at least in 4 distinct points of the interval $(0, \gamma)$. Also, the denominator in (11)

$$1 + \frac{3}{4}(n-1)\frac{(\tilde{\sigma}_{\theta\theta} - \tilde{\sigma}_{rr})^2}{\tilde{\sigma}_e^2} \tag{16}$$

is equal to one for $\theta = \overline{\overline{\theta}}$, whereas it is not influent for $\theta = 0$, as in that case the numerator is zero. It follows that it is convenient to simplify (11) by eliminating the terms (15) and (16). We then make the simplifying hypothesis that the Von Mises stress is constant (which is rigorously true only as n tends to infinite) and we normalize it with respect to its maximum value, determining an approximate solution to the new differential system

$$(1-s)\tilde{\sigma}_{rr} - \tilde{\sigma}_{\theta\theta} + \tilde{\sigma}_{r\theta} = 0 \tag{8}$$

$$\tilde{\sigma}_{\theta\theta,\theta} + (2-s)\tilde{\sigma}_{r\theta} = 0 \tag{9}$$

$$\tilde{u}_{\theta\theta} = \frac{3}{4}\frac{2-sn}{1-sn}(\tilde{\sigma}_{\theta\theta} - \tilde{\sigma}_{rr}) = 0 \tag{10'}$$

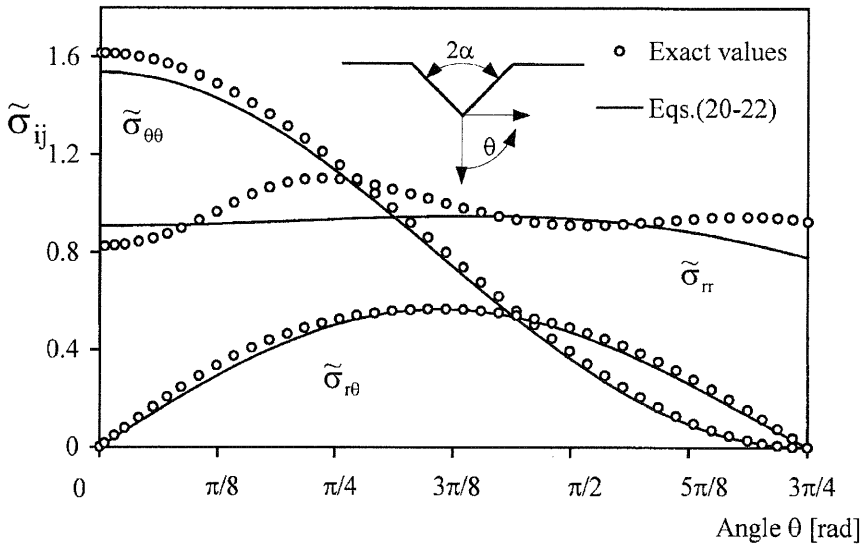

Figure 3. A comparison between exact and approximate stress distributions when $2\alpha = \pi/2$ and n=4.

$$\tilde{\sigma}_{rr,\theta} = \tilde{\sigma}_{\theta\theta,\theta} + 4(1 - sn)\tilde{\sigma}_{r\theta} + \frac{4}{3}(1 - sn)sn\tilde{u}_{\theta} \tag{11'}$$

Equations (10') and (11') are linear with constant coefficients, so that the new formulation admits an analytical solution. It is worth noting that in special case of elastic material (n=1), Equations (10), (11) coincide with the new (10'), (11') and one finds the exact solution due to Williams (1952).

Despite the strong simplification introduced by Equations (10'–11'), the new expressions describe the stress distributions with an acceptable degree of accuracy, at least for $\tilde{\sigma}_{\theta\theta}$ and $\tilde{\sigma}_{r\theta}$ stress components. An example is shown in Figure 3. Generally, the accuracy was seen to increase with the increase of the exponent n and of the opening angle 2α. However, it should be clear that the solution provided by Equations (8, 9, 10' 11') is thought of as a first necessary step in order to build an analytical frame. More refined solutions can be obtained only by adding further terms.

The new system of differential equations (8, 9, 10',11') of the first order can be solved by means of the 4th order associated differential equation for $\tilde{\sigma}_{\theta\theta}$. In particular:

$$\frac{\partial^4\tilde{\sigma}_{\theta\theta}}{\partial\theta^4} - \frac{\partial^2\tilde{\sigma}_{\theta\theta}}{\partial\theta^2}(2s + 2sn + s^2 + s^2n^2 - 4s^2n - 4) - \tilde{\sigma}_{\theta\theta}s^2n(2 - sn)(s - 2) = 0 \tag{17}$$

Hence, after collecting the constants as

$$\xi = 2s + 2sn + s^2 + s^2n^2 - 4s^2n - 4 \quad \zeta = s^2n(2 - sn)(s - 2) \tag{18}$$

the roots of the auxiliary equation (17) result to be:

$$\chi_1 = \frac{\sqrt{\xi + \sqrt{\xi^2 + 4\zeta}}}{2} \qquad \chi_2 = -\frac{\sqrt{\xi + \sqrt{\xi^2 + 4\zeta}}}{2}$$
$$\chi_3 = \frac{\sqrt{\xi - \sqrt{\xi^2 + 4\zeta}}}{2} \qquad \chi_4 = -\frac{\sqrt{\xi - \sqrt{\xi^2 + 4\zeta}}}{2} \tag{19}$$

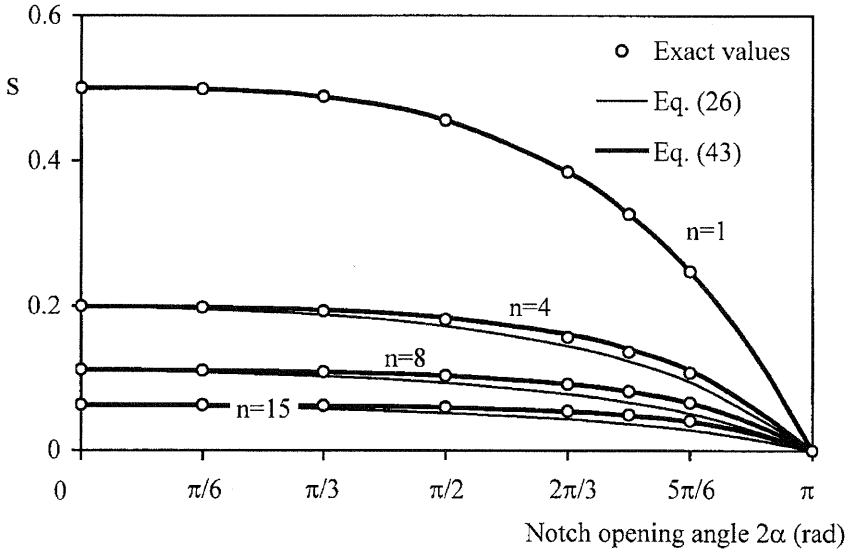

Figure 4. A comparison between exact and approximate values of the eigenvalue s.

For typical values of s and n, the roots (19) are pure complex numbers. Putting $\varphi = |\chi_1| = |\chi_2|$ and $\psi = |\chi_3| = |\chi_4|$, we finally write the resulting stresses as:

$$\tilde{\sigma}_{rr\,lin} = -\frac{(s-2+\varphi^2)[c_1\cos(\varphi\theta)+c_2\sin(\varphi\theta)]+(s-2+\psi^2)[c_3\cos(\psi\theta)+c_4\sin(\psi\theta)]}{(s-2)(s-1)} \tag{20}$$

$$\tilde{\sigma}_{\theta\theta lin} = c_1\cos(\varphi\theta)+c_2\sin(\varphi\theta)+c_3\cos(\psi\theta)+c_4\sin(\psi\theta) \tag{21}$$

$$\tilde{\sigma}_{r\theta lin} = -\frac{\varphi c_1}{s-2}\text{sen}(\varphi\theta)+\frac{\varphi c_2}{s-2}\cos(\varphi\theta)-\frac{\psi c_3}{s-2}\text{sen}(\psi\theta)+\frac{\psi c_4}{s-2}\cos(\psi\theta) \tag{22}$$

Parameters c_1, c_2, c_3 and c_4 can be determined by using the following boundary conditions:

$$\tilde{\sigma}_{r\theta}(0)=0 \quad \tilde{u}_\theta(0)=0 \Rightarrow \tilde{\sigma}_{rr,\theta}(0)=\tilde{\sigma}_{\theta\theta,\theta}(0)=0 \quad \tilde{\sigma}_{\theta\theta}(\gamma)=0 \quad \tilde{\sigma}_{r\theta}(\gamma)=0 \tag{23}$$

Therefore

$$c_2 = c_4 = 0 \tag{24}$$

$$c_3 = -c_1\frac{\varphi\sin(\varphi\gamma)}{\psi\sin(\psi\gamma)} \tag{25}$$

$$\psi\sin(\psi\gamma)\cos(\varphi\gamma)-\varphi\sin(\varphi\gamma)\cos(\psi\gamma)=0 \tag{26}$$

Then, Equation (26) provides the characteristic eigenvalue s of the approximate differential system, and Figure 4 plots approximate and exact values for s. It is evident that the agreement is satisfactory.

Finally, the missing parameter c_1 can be imposed with a normalizing assumption (here we have assumed equal to one the maximum value of the Von Mises equivalent stress).

4. 'A posteriori' correction of the approximate stress solution

The comparison of the proposed solution with respect to the standard HRR solution (or the existing notch stress field solutions) shows that, despite a substantial agreement in the general trends, the errors are not negligible (Figure 3). In order to improve the solution, a second distribution is then superimposed.

For opening angles 2α greater than $\pi/6$ radians, the subsequent terms for stress components seem to be suitable:

$$\tilde{\sigma}_{rr\,corr} = -\frac{s-2+\omega^2}{(s-2)(s-1)} c_5 \cos(\omega\theta) - \frac{c_5}{s-1} \tag{27}$$

$$\tilde{\sigma}_{\theta\theta\,corr} = c_5 \cos(\omega\theta) + c_5 \tag{28}$$

$$\tilde{\sigma}_{r\theta corr} = -\frac{\omega c_5}{s-2} \sin(\omega\theta) \tag{29}$$

Note that, having assumed Equation (28) for the $\tilde{\sigma}_{\theta\theta corr}$ component, expressions (27,29) are then directly obtained from Equations (8,9) which represent the equilibrium conditions.

Equations (27–29) automatically verify the boundary conditions (12) when $\omega = (2m + 1)\pi/\gamma$, m being an integer. In the following sections, we simply let m=1, so that $\omega = 3\pi/\gamma$. In conclusion, the final stress components are:

$$\begin{aligned}\tilde{\sigma}_{rr} = \tilde{\sigma}_{rr\,lin} + \tilde{\sigma}_{rr\,corr} = & -\frac{s-2+\varphi^2}{(s-2)(s-1)} c_1 \cos(\varphi\theta) - \frac{s-2+\psi^2}{(s-2)(s-1)} c_3 \cos(\psi\theta) + \\ & -\frac{s-2+\omega^2}{(s-2)(s-1)} c_5 \cos(\omega\theta) - \frac{c_5}{s-1}\end{aligned} \tag{30}$$

$$\tilde{\sigma}_{\theta\theta} = \tilde{\sigma}_{\theta\theta\,lin} + \tilde{\sigma}_{\theta\theta\,corr} = c_1 \cos(\varphi\theta) + c_3 \cos(\psi\theta) + c_5 \cos(\omega\theta) + c_5 \tag{31}$$

$$\tilde{\sigma}_{r\theta} = \tilde{\sigma}_{r\theta\,lin} + \tilde{\sigma}_{r\theta corr} = -\frac{\varphi c_1}{s-2} \sin(\varphi\theta) - \frac{\psi c_3}{s-2} \sin(\psi\theta) - \frac{\omega c_5}{s-2} \sin(\omega\theta) \tag{32}$$

Obviously Equations (30–32) satisfy both the equilibrium and the boundary conditions. Equations (10, 11), on the other hand, cannot be exactly verified in the entire integration interval; however, it is possible to determine the unknown variable c_5 so that these conditions are fulfilled at least in some points of peculiar interest.

In Equations (30–32) the parameter c_5 or, equivalently, the ratio c_5/c_1 can be derived by imposing a condition on the second derivative of $\tilde{\sigma}_{rr}$ calculated for $\theta = 0$; in particular, we can impose that, on the bisector, the second derivative of $\tilde{\sigma}_{rr}$ is equal when computed either by using the term on the right hand side of Equation (11) or that on the left hand side of the same equation. Due to the boundary conditions, the expression of the second derivative of $\tilde{\sigma}_{rr}$ at the bisector exhibits quite a favorable form:

$$\begin{aligned}\tilde{\sigma}_{rr,\theta,\theta}|_{\theta=0} = & \tilde{\sigma}_{\theta\theta,\theta,\theta}|_{\theta=0} + \frac{4}{n}(1-sn)\tilde{\sigma}_{r\theta,\theta}|_{\theta=0} + \frac{4}{3n}\tilde{\sigma}_e|_{\theta=0}^{1-n}(1-sn)sn\tilde{u}_{\theta,\theta}|_{\theta=0} \\ & \frac{3}{n}(n-1)\frac{\tilde{\sigma}_{rr}|_{\theta=0} - \tilde{\sigma}_{\theta\theta}|_{\theta=0}}{\tilde{\sigma}_e|_{\theta=0}^2}\left(\tilde{\sigma}_{r\theta,\theta}|_{\theta=0}\right)^2\end{aligned} \tag{33}$$

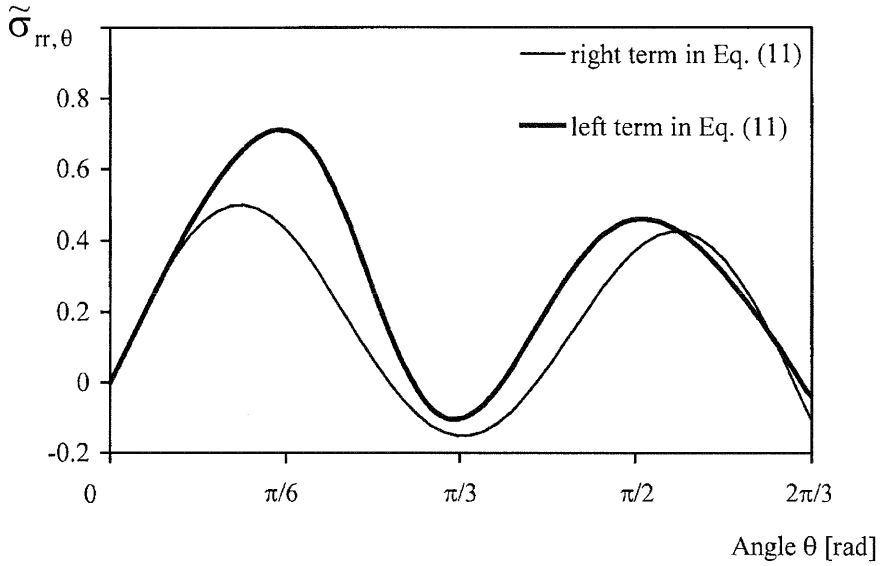

Figure 5. $\tilde{\sigma}_{rr,\theta}$ angular distributions when $2\alpha = \pi/6$ and n=8.

By introducing (30–32) into Equation (33), the final expression is the following:

$$\frac{2n+3sn-4}{n(s-2)}\left(\varphi^2+\frac{c_3}{c_1}\psi^2+\frac{c_5}{c_1}\omega^2\right)+$$

$$s(2-sn)\frac{(s^2-2s+\varphi^2)+\frac{c_3}{c_1}(s^2-2s+\psi^2)+\frac{c_5}{c_1}(3s^2-8s+4+\omega^2)}{(s-1)(s-2)}+$$

$$+\frac{\frac{4(n-1)(1-s)}{n(2-s)}\left(\varphi^2+\frac{c_3}{c_1}\psi^2+\frac{c_5}{c_1}\omega^2\right)^2}{(s^2-2s+\varphi^2)+\frac{c_5}{c_1}(s^2-2s+\psi^2)+\frac{c_5}{c_1}(3s^2-8s+4+\omega^2)}= \tag{34}$$

$$=\frac{\varphi^2+\frac{c_3}{c_1}\psi^2+\frac{c_5}{c_1}\omega^2}{s-1}+\frac{\varphi^4+\frac{c_3}{c_1}\psi^4+\frac{c_5}{c_1}\omega^4}{(s-1)(s-2)}$$

An example of the results obtained is shown in Figure 5, where the predicted values of the $\tilde{\sigma}_{rr,\theta}$, evaluated by the left and the right hand side terms of (11) are plotted.

When the angle 2α is less or equal to $\pi/6$ radians, a first evaluation of the parameter c_5 can be achieved by using the same criterion already proposed for large opening angles.

In order to achieve an adequate accuracy, the additional stress distributions need to be modified as follows:

$$\tilde{\sigma}_{rr\ corr}=\frac{c_5\eta^2[3\cos(\eta\theta)-13.5\cos(\upsilon\theta)+3\sin(\upsilon\theta)\sin(\eta\theta)-3.25\cos(\upsilon\theta)\cos(\eta\theta)]}{(s-2)(s-1)}$$

$$-\frac{c_5\{\cos(\upsilon\theta)[6+\cos(\eta\theta)]-3\cos(\eta\theta)+10\}}{s-1} \tag{35}$$

$$\tilde{\sigma}_{\theta\theta\ corr}=c_5\{\cos(\upsilon\theta)[6+\cos(\eta\theta)]-3\cos(\eta\theta)+10\} \tag{36}$$

$$\tilde{\sigma}_{r\theta\ corr} = \frac{c_5\eta}{s-2}\{\sin(\eta\theta)[3-\cos(\upsilon\theta)] - 1.5\sin(\upsilon\theta)[6+\cos(\eta\theta)]\} \tag{37}$$

where $\eta = 2\pi/\gamma$ and $\upsilon = 3\pi/\gamma$. Once again, Equation (36) is our proposal whereas Equations (35, 37) are consequences of Equation (36).

Then the complete formulation is:

$$\begin{aligned}\tilde{\sigma}_{rr} = \tilde{\sigma}_{rr\ lin} + \tilde{\sigma}_{rr\ corr} = &-\frac{s-2+\varphi^2}{(s-2)(s-1)}c_1\cos(\varphi\theta) - \frac{s-2+\psi^2}{(s-2)(s-1)}c_3\cos(\psi\theta)+\\ &+\frac{c_5\eta^2]3\cos(\eta\theta) - 13.5\cos(\upsilon\theta) + 3\sin(\upsilon\theta)\sin(\eta\theta) - 3.25\cos(\upsilon\theta)\cos(\eta\theta)]}{(s-2)(s-1)}+\\ &-\frac{c_5\{\cos(\upsilon\theta)[6+\cos(\eta\theta)] - 3\cos(\eta\theta) + 10\}}{s-1}\end{aligned} \tag{38}$$

$$\begin{aligned}\tilde{\sigma}_{\theta\theta} = \tilde{\sigma}_{\theta\theta\ lin} + \tilde{\sigma}_{\theta\theta\ corr} = &\ c_1\cos(\varphi\theta)+\\ &+c_3\cos(\psi\theta) + c_5\{\cos(\upsilon\theta)[6+\cos(\eta\theta)] - 3\cos(\eta\theta) + 10\}\end{aligned} \tag{39}$$

$$\begin{aligned}\tilde{\sigma}_{r\theta} = \tilde{\sigma}_{r\theta\ lin} + \tilde{\sigma}_{r\theta\ corr} = &-\frac{\varphi c_1}{s-2}\sin(\varphi\theta) - \frac{\psi c_3}{s-2}\sin(\psi\theta)+\\ &\frac{c_5\eta}{s-2}\{\sin(\eta\theta)[3-\cos(\upsilon\theta)] - 1.5\sin(\upsilon\theta)[6+\cos(\eta\theta)]\}\end{aligned} \tag{40}$$

Following the same criterion previously used for large V notch cases, and taking advantage of Equations (38–40), condition (33) can be expressed as follows:

$$\begin{aligned}&\frac{4-3sn-2n}{n(s-2)}\left(-\varphi^2 - \frac{c_3}{c_1}\psi^2 - \frac{c_5}{c_1}13.75\eta^2\right) +\\ &\frac{4\dfrac{s-1}{s-2}\dfrac{n-1}{n}\left(\varphi^2 + \dfrac{c_3}{c_1}\psi^2 + \dfrac{c_5}{c_1}13.75\eta^2\right)^2}{(s^2-2s)\left(1+\dfrac{c_3}{c_1}\right) + \varphi^2 + \dfrac{c_3}{c_1}\psi^2 + \dfrac{c_5}{c_1}(14s^2 + 13.75\eta^2 - 28s)}+\\ &\frac{s(2-sn)}{(s-1)(s-2)}\left[(s^2-2s)\left(1+\frac{c_3}{c_1}\right) + \varphi^2 + \frac{c_3}{c_1}\psi^2 + \frac{c_5}{c_1}(14s^2 + 13.75\eta^2 - 28s)\right] =\\ &= \frac{\varphi^2 + \dfrac{c_3}{c_1}\psi^2}{s-1} + \frac{\varphi^4 + \dfrac{c_3}{c_1}\psi^4}{(s-1)(s-2)} + \frac{c_5}{c_1}\left[\frac{46.9375\eta^4}{(s-1)(s-2)} + \frac{13.75\eta^2}{(s-1)}\right]\end{aligned} \tag{41}$$

The parameter c_5 can then be determined by solving Equation (41).

In any case, a better agreement between exact values an analytical predictions can be achieved by increasing the c_5/c_1 ratio to c_5^*/c_1. The new parameter c_5^* can be evaluated by performing a best fitting between the left and right hand side terms of Equation (11) over the range (0-$\gamma/3$). Such a range represents in fact the region where the maximum variation of $\tilde{\sigma}_{rr,\theta}$ takes place.

This objective can be reached by introducing the integral mean values of the terms in Equation (11). Solving the close-form integrals, the best-fitting condition can be given as follows:

Table 1a. Parameter values in Equations (30–32).

2α	n	s	φ	ψ	ω	c_3/c_1	c_5/c_1
	4	0.188	0.4072	1.3867	3.6	0.5476	0.0196
$\pi/3$	8	0.102	0.3300	1.3096	3.6	0.6772	0.0230
	15	0.0565	0.2594	1.2628	3.6	0.7888	0.0250
	4	0.172	0.3662	1.4547	4	0.6778	0.0129
$\pi/2$	8	0.0925	0.2890	1.4035	4	0.7878	0.0156
	15	0.0510	0.2232	1.3733	4	0.8687	0.0171
	4	0.144	0.2989	1.5655	4.5	0.8182	0.0075
$2\pi/3$	8	0.077	0.231	1.538	4.5	0.888	0.0093
	15	0.0424	0.1763	1.5214	4.5	0.9335	0.0103
	4	0.123	0.2514	1.6419	4.8	0.8836	0.0053
$3\pi/4$	8	0.0657	0.1932	1.6241	4.8	0.9300	0.0066
	15	0.0362	0.1468	1.6137	4.8	0.9591	0.0077
	4	0.0941	0.1906	1.7361	5.143	0.9403	0.0033
$5\pi/6$	8	0.0506	0.1462	1.7270	5.143	0.9646	0.0041
	15	0.0279	0.1110	1.7215	5.143	0.9795	0.00457

Table 1b. Parameter values in Equations (38–40).

2α	n	s	φ	ψ	η	υ	c_3/c_1	c_5/c_1	c_5^*/c_1
	4	0.199	0.4398	1.3328	2	3	0.3747	0.00466	0.00272
0	8	0.111	0.3765	1.2075	2	3	0.4758	0.00489	0.00483
	15	0.0624	0.3093	1.122	2	3	0.6081	0.00505	0.00675
	4	0.196	0.4298	1.3493	2.182	3.2727	0.4444	0.00324	0.00276
$\pi/6$	8	0.108	0.3584	1.2466	2.182	3.2727	0.5693	0.00355	0.00486
	15	0.0601	0.2877	1.1810	2.182	3.2727	0.6994	0.00375	0.00670

$$\frac{\tilde{\sigma}_{rr}\left(\frac{\gamma}{3}\right) - \tilde{\sigma}_{rr}(0) + \tilde{\sigma}_{\theta\theta}(0) - \tilde{\sigma}_{\theta\theta}\left(\frac{\gamma}{3}\right)}{\int_0^{\frac{\gamma}{3}} \frac{4(1-sn)(\tilde{\sigma}_{r\theta} + \frac{4}{3}\tilde{\sigma}_e^{1-n}(1-sn)sn\tilde{u}_\theta - 3(n-1)\frac{\tilde{\sigma}_{rr}-\tilde{\sigma}_{\theta\theta}}{\tilde{\sigma}_e^2}\tilde{\sigma}_{r\theta}\tilde{\sigma}_{r\theta,\theta}}{1+\frac{3}{4}(n-1)\frac{(\tilde{\sigma}_{\theta\theta}-\tilde{\sigma}_{rr})^2}{\tilde{\sigma}_e^2}} d\theta} = 1 \tag{42}$$

For three values of the exponent n and six values of the opening angle 2α, Table 1a,b summarizes values for s and the other parameters. Table 2a,b gives all the coefficients present in stress expressions (30–32) or (38–40) in order to make their use immediate, at least in all the cases considered here.

Table 2a. Synthesis of coefficients valid for Equations (30–32).

2α	n	$\frac{s-2+\varphi^2}{(s-2)(s-1)}$	$\frac{s-2+\psi^2}{(s-2)(s-1)}\frac{c_3}{c_1}$	$\frac{s-2+\omega^2}{(s-2)(s-1)}\frac{c_5}{c_1}$	$\frac{c_5}{c_1(s-1)}$	$\frac{\varphi}{s-2}$	$\frac{\psi}{s-2}\frac{c_3}{c_1}$	$\frac{\omega}{s-2}\frac{c_5}{c_1}$
	4	−1.119	0.041	0.148	−0.024	−0.225	−0.419	−0.039
$\pi/3$	8	−1.050	−0.073	0.149	−0.026	−0.174	−0.467	−0.044
	15	−1.023	−0.150	0.150	−0.026	−0.133	−0.513	−0.046
	4	−1.119	0.129	0.121	−0.016	−0.200	−0.539	−0.028
$\pi/2$	8	−1.054	0.028	0.127	−0.017	−0.152	−0.580	−0.033
	15	−1.027	−0.030	0.130	−0.018	−0.115	−0.612	−0.035
	4	−1.112	0.306	0.087	−0.009	−0.161	−0.690	−0.018
$2\pi/3$	8	−1.053	0.221	0.096	−0.010	−0.120	−0.710	−0.022
	15	−1.028	0.178	0.101	−0.011	−0.090	−0.725	−0.024
	4	−1.102	0.440	0.068	−0.006	−0.134	−0.773	−0.014
$3\pi/4$	8	−1.050	0.362	0.077	−0.007	−0.100	−0.781	−0.016
	15	−1.026	0.324	0.086	−0.008	−0.075	−0.788	−0.019
	4	−1.083	0.604	0.047	−0.004	−0.100	−0.857	−0.009
$5\pi/6$	8	−1.042	0.538	0.054	−0.004	−0.075	−0.855	−0.011
	15	−1.022	0.507	0.058	−0.005	−0.056	−0.855	−0.012

Table 2b. Synthesis of coefficients valid for Equations (38–40).

2α	n	$\frac{s-2+\varphi^2}{(s-2)(s-1)}$	$\frac{s-2+\psi^2}{(s-2)(s-1)}\frac{c_3}{c_1}$	$\frac{c_5^*\eta^2}{c_1(s-2)(s-1)}$	$\frac{c_5^*}{c_1(s-1)}$	$\frac{\varphi}{s-2}$	$\frac{\psi}{s-2}\frac{c_3}{c_1}$	$\frac{\omega}{s-2}\frac{c_5}{c_1}$
	4	−1.114	−0.006	0.00717	−0.00323	−0.244	−0.277	−0.00287
0	8	−1.040	−0.122	0.01096	−0.00518	−0.199	−0.304	−0.00487
	15	−1.014	−0.227	0.01423	−0.00689	−0.160	−0.352	−0.00667
	4	−1.116	0.005	0.00873	−0.00331	−0.238	−0.332	−0.00322
$\pi/6$	8	−1.045	−0.114	0.01325	−0.00526	−0.189	−0.375	−0.00541
	15	−1.019	−0.209	0.01696	−0.00691	−0.148	−0.426	−0.00730

5. Results

The accuracy of the obtained solutions is checked against previous numerical results obtained with a special purposed code generated within the Matlab® environment for studying stress fields with localized plasticity (Lazzarin et al., 2001).

Tables 3, 4 and 5 report stress values in different points of the interval $(0, \gamma)$ and for several values of n and 2α. In particular, the columns on the left hand side give the exact values, whereas the approximate results are on the right hand side. It is quite evident that the degree of accuracy of the approximate closed form solution is remarkably high, in the entire range of notch angles and for the values of n of greater significance (i.e. from 4 to 15). Moreover it is

Table 3. A comparison between exact values (on the left) and approximate values (on the right) of the stress distributions (n=4).

θ	n=4	$2\alpha = 0$	$2\alpha = \pi/6$	$2\alpha = \pi/3$	$2\alpha = \pi/2$	$2\alpha = 2\pi/3$	$2\alpha = 3\pi/4$	$2\alpha = 5\pi/6$
	σ_{rr}	1.67–1.54	1.39–1.36	1.11–1.10	0.83–0.85	0.54–0.58	0.40–0.43	0.26–0.29
0	$\sigma_{\theta\theta}$	2.10–2.04	1.96–1.95	1.79–1.83	1.62–1.64	1.44–1.45	1.36–1.37	1.28–1.29
	$\sigma_{r\theta}$	0–0	0–0	0–0	0–0	0–0	0–0	0–0
	σ_{rr}	1.78–1.67	1.60–1.56	1.36–1.37	1.06–1.06	0.78–0.77	0.62–0.62	0.46–0.47
$\cong \gamma/4$	$\sigma_{\theta\theta}$	1.74–1.64	1.63–1.61	1.46–1.49	1.36–1.39	1.19–1.21	1.13–1.15	1.08–1.09
	$\sigma_{r\theta}$	0.44–0.48	0.44–0.46	0.46–0.49	0.44–0.44	0.45–0.44	0.44–0.43	0.43–0.42
	σ_{rr}	1.27–1.26	1.20–1.23	1.08–1.13	1.00–1.02	0.88–0.86	0.82–0.79	0.75–0.72
$\cong \gamma/2$	$\sigma_{\theta\theta}$	1.02–0.89	0.96–0.92	0.83–0.84	0.80–0.82	0.73–0.74	0.64–0.66	0.62–0.63
	$\sigma_{r\theta}$	0.56–0.54	0.56–0.56	0.56–0.55	0.57–0.57	0.57–0.57	0.57–0.57	0.57–0.57
	σ_{rr}	0.88–0.75	0.89–0.82	0.89–0.86	0.91–0.90	0.94–0.92	0.97–0.96	0.98–0.97
$\cong 3\gamma/4$	$\sigma_{\theta\theta}$	0.29–0.25	0.29–0.28	0.24–0.25	0.25–0.26	0.23–0.22	0.18–0.18	0.18–0.18
	$\sigma_{r\theta}$	0.41–0.34	0.42–0.39	0.40–0.40	0.42–0.43	0.42–0.43	0.39–0.40	0.39–0.39
	σ_{rr}	0.60–0.51	0.73–0.62	0.83–0.87	0.93–0.95	1.01–1.03	1.06–1.07	1.10–1.11
γ	$\sigma_{\theta\theta}$	0–0	0–0	0–0	0–0	0–0	0–0	0–0
	$\sigma_{r\theta}$	0–0	0–0	0–0	0–0	0–0	0–0	0–0

Table 4. A comparison between exact values (on the left) and approximate values (on the right) of the stress distributions (n=8).

θ	n=8	$2\alpha = 0$	$2\alpha = \pi/6$	$2\alpha = \pi/3$	$2\alpha = \pi/2$	$2\alpha = 2\pi/3$	$2\alpha = 3\pi/4$	$2\alpha = 5\pi/6$
	σ_{rr}	1.71–1.70	1.43–1.43	1.14–1.16	0.85–0.88	0.56–0.60	0.42–0.45	0.27–0.31
0	$\sigma_{\theta\theta}$	2.42–2.43	2.21–2.24	1.99–2.00	1.76–1.76	1.54–1.53	1.44–1.43	1.33–1.33
	$\sigma_{r\theta}$	0–0	0–0	0–0	0–0	0–0	0–0	0–0
	σ_{rr}	1.95–1.93	1.74–1.74	1.46–1.40	1.13–1.08	0.81–0.78	0.63–0.63	0.46–0.47
$\cong \gamma/4$	$\sigma_{\theta\theta}$	1.97–1.96	1.84–1.87	1.63–1.64	1.48–1.48	1.29–1.30	1.22–1.23	1.14–1.15
	$\sigma_{r\theta}$	0.47–0.51	0.47–0.48	0.49–0.50	0.47–0.45	0.46–0.44	0.44–0.42	0.42–0.44
	σ_{rr}	1.35–1.38	1.20–1.24	1.08–1.11	0.98–0.98	0.85–0.84	0.80–0.77	0.73–0.70
$\cong \gamma/2$	$\sigma_{\theta\theta}$	1.23–1.19	1.07–1.1	0.96–0.95	0.87–0.87	0.75–0.75	0.72–0.72	0.68–0.68
	$\sigma_{r\theta}$	0.57–0.57	0.57–0.57	0.57–0.57	0.57–0.57	0.57–0.58	0.58–0.58	0.58–0.58
	σ_{rr}	0.83–0.77	0.82–0.77	0.84–0.81	0.86–0.84	0.90–0.88	0.92–0.90	0.93–0.92
$\cong 3\gamma/4$	$\sigma_{\theta\theta}$	0.42–0.41	0.34–0.36	0.30–0.30	0.28–0.28	0.22–0.21	0.22–0.21	0.21–0.21
	$\sigma_{r\theta}$	0.48–0.46	0.46–0.47	0.45–0.45	0.45–0.44	0.42–0.42	0.43–0.43	0.43–0.43
	σ_{rr}	0.79–0.82	0.86–0.96	0.92–0.91	0.97–0.96	1.03–1.01	1.06–1.05	1.09–1.08
γ	$\sigma_{\theta\theta}$	0–0	0–0	0–0	0–0	0–0	0–0	0–0
	$\sigma_{r\theta}$	0–0	0–0	0–0	0–0	0–0	0–0	0–0

Table 5. A comparison between exact values (on the left) and approximate values (on the right) of the stress distributions (n=15).

θ	n=15	$2\alpha = 0$	$2\alpha = \pi/6$	$2\alpha = \pi/3$	$2\alpha = \pi/2$	$2\alpha = 2\pi/3$	$2\alpha = 3\pi/4$	$2\alpha = 5\pi/6$
	σ_{rr}	1.75–1.78	1.46–1.47	1.13–1.19	0.87–0.90	0.58–0.61	0.43–0.46	0.28–0.31
0	$\sigma_{\theta\theta}$	2.62–2.56	2.37–2.42	2.09–2.08	1.86–1.81	1.61–1.57	1.49–1.46	1.37–1.35
	$\sigma_{r\theta}$	0–0	0–0	0–0	0–0	0–0	0–0	0–0
	σ_{rr}	2.08–2.09	1.82–1.86	1.48–1.40	1.19–1.09	0.85–0.79	0.65–0.63	0.50–0.49
$\cong \gamma/4$	$\sigma_{\theta\theta}$	2.13–2.17	1.93–1.98	1.73–1.73	1.54–1.51	1.33–1.32	1.26–1.25	1.14–1.14
	$\sigma_{r\theta}$	0.51–0.52	0.51–0.50	0.50–0.49	0.49–0.46	0.47–0.45	0.44–0.42	0.45–0.43
	σ_{rr}	1.39–1.42	1.26–1.29	1.09–1.11	0.97–0.96	0.84–0.82	0.79–0.76	0.72–0.70
$\cong \gamma/2$	$\sigma_{\theta\theta}$	1.33–1.35	1.20–1.25	1.02–1.03	0.91–0.89	0.77–0.76	0.75–0.74	0.66–0.65
	$\sigma_{r\theta}$	0.57–0.57	0.57–0.57	0.58–0.58	0.58–0.58	0.58–0.58	0.58–0.58	0.58–0.58
	σ_{rr}	0.78–0.76	0.78–0.75	0.81–0.79	0.85–0.81	0.88–0.86	0.89–0.87	0.94–0.92
$\cong 3\gamma/4$	$\sigma_{\theta\theta}$	0.47–0.49	0.40–0.45	0.31–0.32	0.30–0.29	0.23–0.21	0.24–0.22	0.19–0.18
	$\sigma_{r\theta}$	0.52–0.53	0.50–0.53	0.47–0.46	0.47–0.45	0.44–0.42	0.44–0.43	0.41–0.41
	σ_{rr}	0.92–1.02	0.95–1.12	0.99–0.93	1.02–0.96	1.05–1.00	1.07–1.03	1.10–1.07
γ	$\sigma_{\theta\theta}$	0–0	0–0	0–0	0–0	0–0	0–0	0–0
	$\sigma_{r\theta}$	0–0	0–0	0–0	0–0	0–0	0–0	0–0

useful to remember that the solution coincides with the Williams solution in the linear elastic case (n=1).

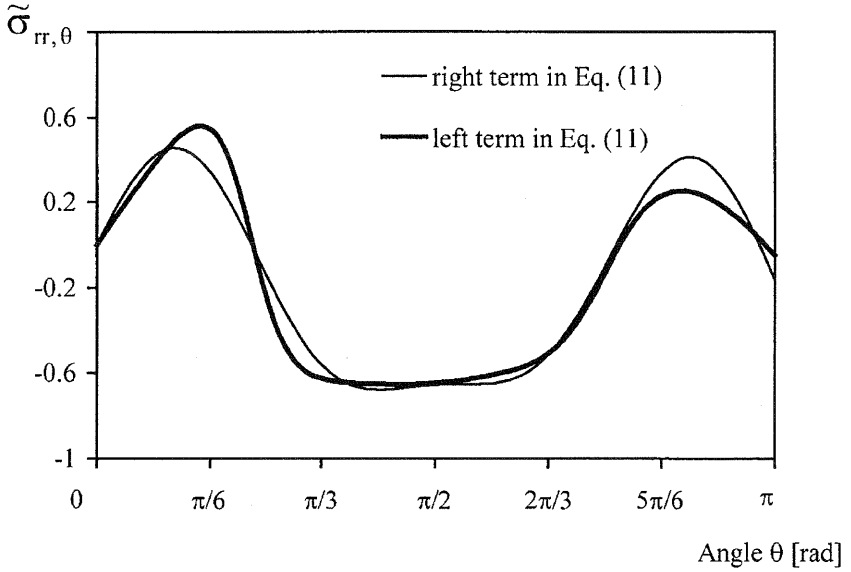

Figure 6. $\tilde{\sigma}_{rr,\theta}$ angular distributions when $2\alpha = 0$ and n=15.

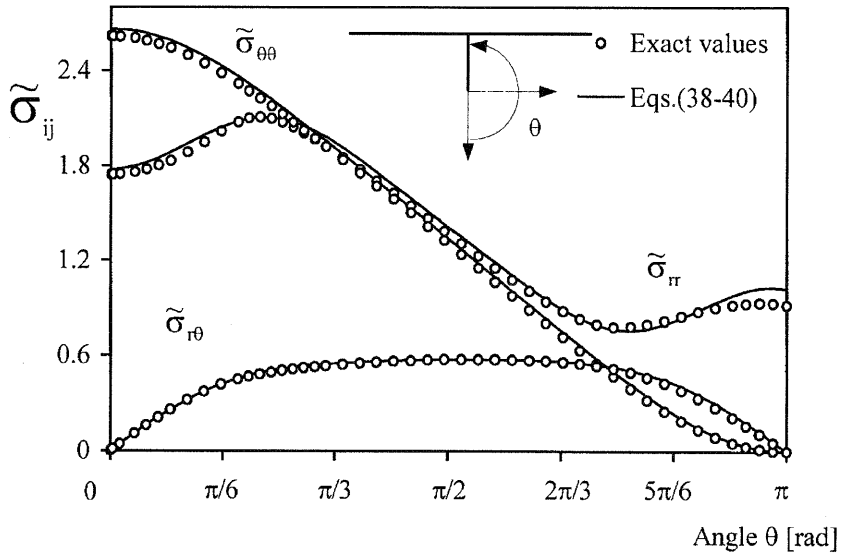

Figure 7. Stress field distributions for the crack-case when n=15.

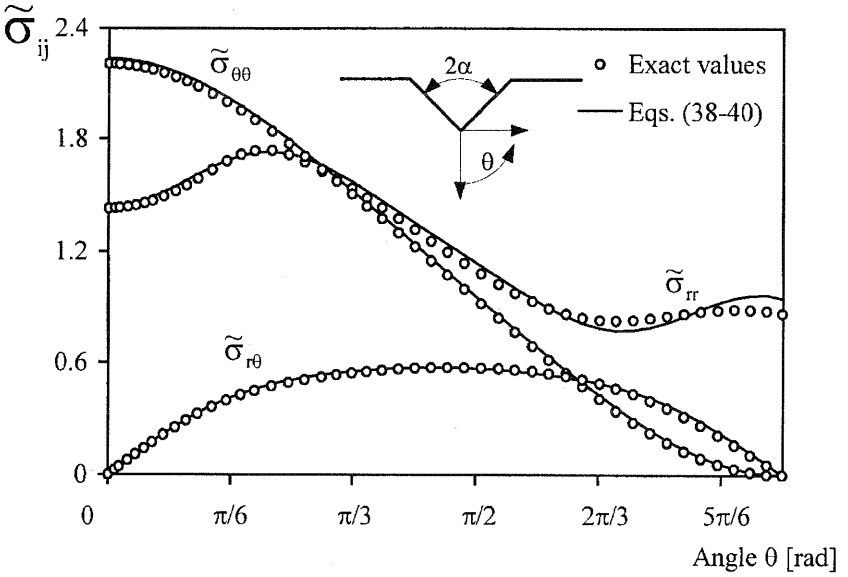

Figure 8. Stress field distributions when $2\alpha = \pi/6$ and n=8.

Table 6 reports the values of the eigenvalue s as given by Equation (26). The data demonstrate a very satisfactory accuracy when the notch opening angle is close to zero, while predictions get less accurate in relative terms when 2α and n increase so that s tends towards zero. An improved calculation of the eigenvalue s, can be obtained by correcting the predicted value:

$$s^* = \frac{s}{g(n, 2\alpha)} \tag{43}$$

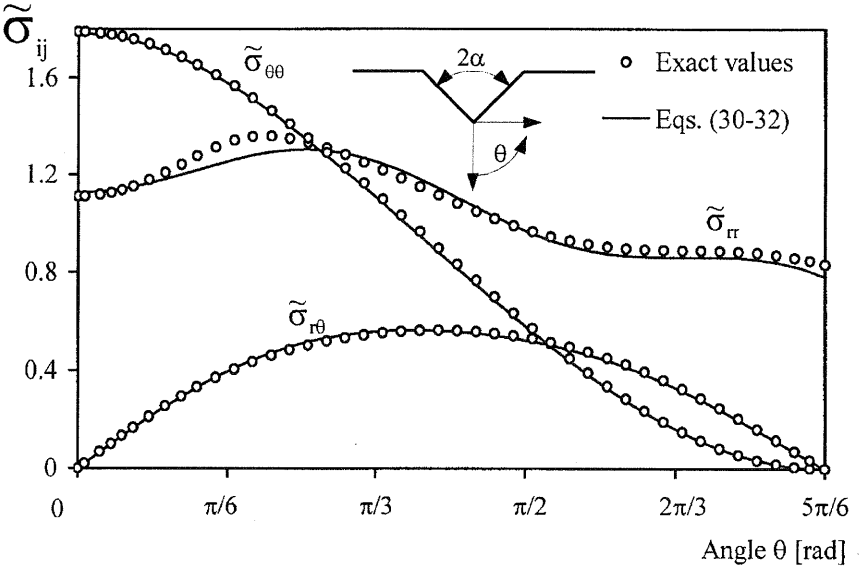

Figure 9. Stress field distributions when $2\alpha = \pi/3$ and n=4.

Table 6. A comparison between exact and approximate values of the eigenvalue s

n		$2\alpha = 0$	$2\alpha = \pi/6$	$2\alpha = \pi/3$	$2\alpha = \pi/2$	$2\alpha = 2\pi/3$	$2\alpha = 3\pi/4$	$2\alpha = 5\pi/6$
1	Exact value	0.5	0.4985	0.4878	0.4555	0.3843	0.3264	0.2483
	Exact value	0.2	0.1983	0.1931	0.181	0.1562	0.1357	0.1068
	Eq.(26)	0.1991	0.1956	0.1876	0.172	0.144	0.1226	0.0941
4	Eq.(43)	0.1991	0.1983	0.1944	0.1840	0.1605	0.1401	0.1106
	Eq.(45)	0.2	0.1994	0.1951	0.1822	0.1537	0.1306	0.0992
	Eq.(46)	0.2	0.1985	0.1931	0.1809	0.1555	0.1346	0.1059
	Exact value	0.1111	0.1101	0.1079	0.1025	0.0909	0.0807	0.0655
	Eq.(26)	0.1108	0.1076	0.1019	0.0925	0.077	0.0657	0.0506
8	Eq.(43)	0.1108	0.1098	0.1076	0.1025	0.0911	0.0809	0.0652
	Eq.(45)	0.1111	0.1108	0.1084	0.1012	0.0854	0.0725	0.0551
	Eq.(46)	0.1111	0.1105	0.1080	0.1023	0.0897	0.0789	0.0638
	Exact value	0.0625	0.0621	0.061	0.0587	0.0536	0.0486	0.0406
	Eq.(26)	0.0624	0.0601	0.0565	0.0510	0.0424	0.0362	0.0279
15	Eq.(43)	0.0624	0.0617	0.0607	0.0584	0.0531	0.0478	0.0394
	Eq.(45)	0.0625	0.0623	0.0610	0.0569	0.0480	0.0408	0.0310
	Eq.(46)	0.0625	0.0622	0.0613	0.0588	0.0528	0.0475	0.0398

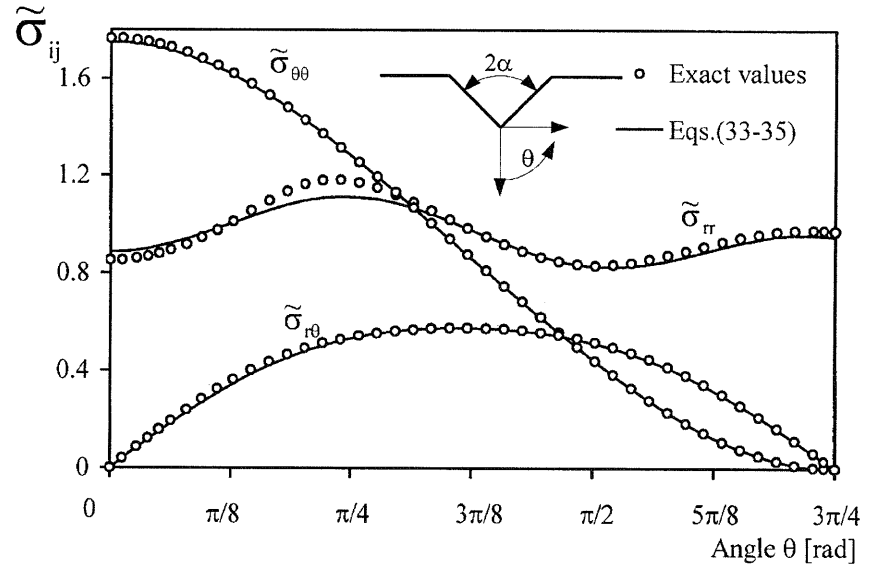

Figure 10. Stress field distributions when $2\alpha = \pi/2$ and n=8.

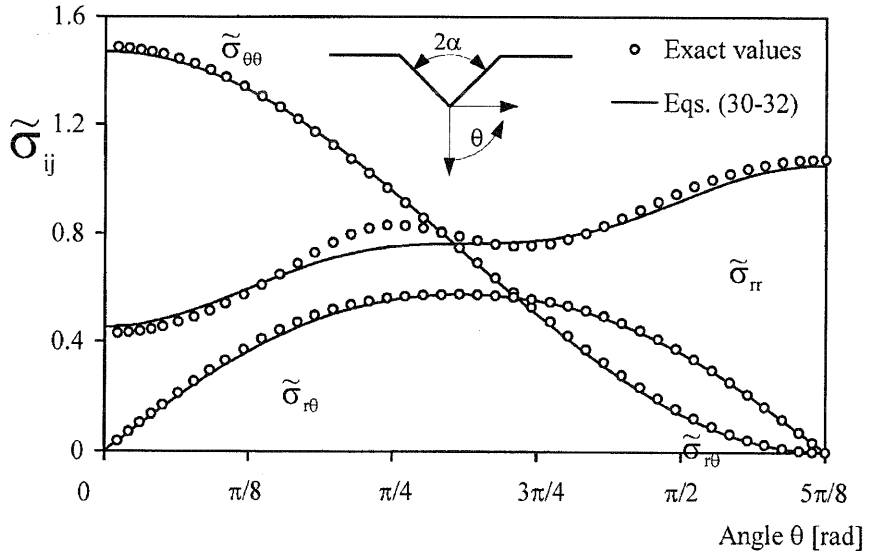

Figure 11. Stress field distributions when $2\alpha = 3\pi/4$ and n=15.

where g is a function of the angle 2α (in radians):

$$g(n, 2\alpha) = 1 + \nu \ln(n)[\lambda 2\alpha + \mu(2\alpha)^2] \tag{44}$$

Parameters ν, λ and μ in Equation (44) were calculated via best fitting tecniques. They results to be $\nu = 0.78$, $\lambda = -0.01670$ and $\mu = -0.01374$.

Figure 4 shows the value of eigenvalue s calculated by exact numerical approach and by relations (23) and (43).

Other approximate expressions to estimate s were proposed by Kuang and Xu (1987):

$$s^{**} = 2\frac{1-\lambda_1}{n+1} \tag{45}$$

$$s^{***} = 2\frac{1-\lambda_1}{n+1} + \frac{(n-1/n) - 6.52589\cot(\alpha)(1-1/n)}{n+4+25\{1-\cos(\alpha)+[1-\cos(\alpha)]^3\}} \cdot \frac{1-2(1-\lambda_1)}{n+1} \tag{46}$$

where, λ_1 is the elastic mode I eigenvalue. A comparison between exact values and the data resulting from Equations (29), (47) and (45–46) is reported in Table 6. It is useful to note that in Equation (46) the number −6.52589 substitutes the number +6.52589 present in the original paper. However the authors have assured that Equation (46) matches all the data tabled therein.

Figures 7–8 show angular distributions for the crack and $\pi/6$ V notch obtained by using the c_5^* parameter. Figures 9–11 show angular distributions for V-notches having an opening angle 2α ranging from $\pi/3$ to $3\pi/4$ radians. In all cases the agreement between approximated expressions and exact values for stresses was found to be very good. This always holds true for n equal to or less than 15. It is remarked that the components $\tilde{\sigma}_{\theta\theta}$ and $\tilde{\sigma}_{r\theta}$ are always more accurate than the $\tilde{\sigma}_{rr}$, and this was also noticed by Kuang e Xu (1987) for ideally plastic materials.

6. Conclusions

This paper has obtained two approximate closed form solutions for the J_2 deformation theory elasto-plastic stress fields in V-notches subjected to mode I loading. The former solution is valid for V-notch opening angles ranging from $\pi/6$ radians to $5\pi/6$ radians, the later for angles ranging from zero to $\pi/6$ radians. Starting from a simplified differential system where non linear equations are modified in order to achieve a closed-form solution, an *a posteriori* correction was suggested in order to improve the respect of the compatibility conditions. Eigenvalues and angular stress function have been shown to be very accurate in the presence of a hardening exponent n equal to or less than 15. In the limit of n=1, elastic material, the solution coincides with Williams' celebrated solution (Williams, 1952).

All equations reported in the paper have been rewritten by using a commercial code. If requested, the corresponding authors will send it to all the readers interested.

References

Chen D.H. and Ushijima K. (2000) Elastic-plastic stress singularity near the tip of a V-notch. *International Journal of Fracture* **106**, 117–134.

Hutchinson J.W. (1968) Singular behaviour at the end of a tensile crack in a hardening material. *Journal of Mechanics and Physics of Solids* **16**, 13–31.

Kuang Z.B., Xu X.P. (1987) Stress and strain fields at the tip of a V - notch in a power - law hardening material. *International Journal of Fracture* **35**, 39–53.

Lazzarin P., Zambardi R., Livieri, P. (2001) Plastic Notch Stress Intensity Factors for Large V-Shaped Notches under Mixed Load Conditions. *International Journal of Fracture* **107**, 361–377.

Ponte Castañeda P. (1985) Asymptotic fields in steady crack growth with linear strain-hardening. *Journal of the Mechanics and Physics of Solids* **35**, 227–268.

Rice J.R. (1968) A path independent integral and the approximate analysis of strain concentration by notches and cracks. *Journal of Applied Mechanics* **35**, 379–386.

Rice J.R., Rosengren, G.F. (1968) Plane strain deformation near a crack tip in a power - law hardening material. *Journal of Mechanics and Physics of Solids* **16**, 1–12.

Sharma S.M. and Aravas N. (1991) Determination of higher-order terms in asymptotic elastoplastic crack tip solutions. *Journal of the Mechanics and Physics of Solids* **39**, 1043–1072.

Sharma S.M. and Aravas N. (1993) On the development of variable-separable asymptotic elastoplastic solutions for interfacial cracks. *International Journal of Solids and Structures* **30**, 695–723.

Xia L., Wang T. (1993) Singular behavior near the tip of a sharp V - notch in a power - hardening material. *International Journal of Fracture* **59**, 83–93.

Yuan H., Lin G. (1994) Analysis of elastoplastic sharp notches. *International Journal of Fracture* **67**, 187–216.

Zhang N., Joseph P.F. (1998) A nonlinear finite element eingenanalysis of singular plane stress fields in bimaterial wedges including complex eingenvalues. *International Journal of Fracture* **90**, 175–207.

Williams M.L. (1952) Stress singularities resulting from various boundary conditions in angular corners of plates in tension. *Journal of Applied Mechanics* **19**, 526–528.